

LOFAR as a probe of the sources of cosmological reionization

Saleem Zaroubi^{1*} and Joseph Silk²

¹*Kapteyn Astronomical Institute, University of Groningen, Landleven 12, 9747 AG Groningen, the Netherlands*

²*Astrophysics Department, University of Oxford, Keble Road, Oxford OX1 3RH*

Accepted 2005 March 30. Received 2005 February 23; in original form 2004 December 3

ABSTRACT

We propose use of the thickness of the ionization front as a discriminant between alternative modes of reionization in the early Universe, by stars or by miniquasars. Assuming a photoionization–recombination balance, we find that for miniquasar sources the transition from neutral to ionized intergalactic medium is extended and has two features. The first is a sudden steep increase in the neutral fraction with a typical width of 5–10 comoving megaparsecs, depending on the miniquasar power. The second feature is a long wing that represents a much slower transition from a neutral fraction of ≈ 0.8 to 1. The angular resolution of LOFAR is expected to resolve these scales and will, therefore, play an important role in discriminating the hard sources of ionizing photons from the stellar ones.

Key words: quasars: general – cosmology: theory – diffuse radiation – large-scale structure of Universe – radio lines: general.

1 INTRODUCTION

The Universe is generally considered to have become reionized at a redshift larger than 10. This result, coming from analysis of the *Wilkinson Microwave Anisotropy Probe* (*WMAP*) polarization power spectrum (Kogut et al. 2003; Spergel et al. 2003), came as a surprise, in the context of earlier studies of the Gunn–Peterson effect inferred to be present at $z \sim 6$ (e.g. Fan et al. 2002) and of the high temperature of the intergalactic medium (IGM) at $z \sim 3$ (Theuns et al. 2002; Hui & Haiman 2003). Given this result, the ionizing sources cannot be known quasars or normal galaxies. Rather, recourse must be had to Population III stars or to miniquasars, both of which represent hypothetical but plausible populations of the first objects in the Universe, and which are significant sources of ionizing photons.

The impact of stellar sources has been studied by many authors (e.g. Cen 2003; Ciardi, Ferrara & White 2003; Haiman & Holder 2003; Sokasian et al. 2003; Somerville & Livio 2003; Wyithe & Loeb 2004). These studies find in general that in order to provide enough ionizing flux at or before $z = 15$, for the usual scale-invariant primordial density fluctuation power spectrum, one needs Population III stars, which provide about 20 times more ionizing photons per baryon than Population II (Bromm, Kudritzki & Loeb 2001; Schaerer 2002), or an initial mass function (IMF) that initially is dominated by high-mass stars (Daigne et al. 2004). This is in agreement with recent numerical simulations of the formation of the first stars from primordial molecular clouds, which suggest that the first metal-free stars were predominantly very massive, $m_* \gtrsim 100 M_\odot$ (Abel, Bryan & Norman 2000, 2002; Bromm, Coppi & Larson 2002).

Theoretically, there is some tension between the low amplitude of the fluctuations as interpreted from low-redshift data (e.g. Croft et al. 2002, Zaroubi et al., in preparation) and the early ionization observed by the *WMAP* satellite. Most of the theoretical and numerical results mentioned earlier require a somewhat higher value of the fluctuation amplitude and would have a harder time satisfying all of the observational constraints with lower amplitude ($\sigma_8 \approx 0.8$). It is unclear whether this tension is caused by the theoretical uncertainties in the physical details of the ionization process, or whether it is an indication of the existence of a non-standard cosmological model in which non-linear structures assemble earlier than in the normal Λ cold dark matter scenario (e.g. Sugiyama, Zaroubi & Silk 2004; Avelino & Liddle 2004).

Miniquasars have also been considered as a significant ionizing source (e.g. Oh 2000, 2001; Ricotti & Ostriker 2004a,b; Madau et al. 2004; Dijkstra, Haiman & Loeb 2004). These latter are as plausible as Population III stars, the nucleosynthetic traces of which have not yet been seen even in the most metal-poor halo stars or in the high- z Lyman α forest, in view of the correlation between central black hole mass and spheroid velocity dispersion (Gebhardt et al. 2000; Ferrarese & Merritt 2000; Ferrarese 2002). This correlation demonstrates that seed black holes must have been present before spheroid formation. Indeed, recent observations of a quasar host galaxy at $z = 6.42$ (Walter et al. 2004) (and other quasars) suggest that supermassive black holes were in place and pre-dated the formation of the spheroid. Theory suggests that the seeds from which the supermassive black hole formed amounted to at least $1000 M_\odot$ and were in place before $z \sim 10$ (Madau & Rees 2001; Islam, Taylor & Silk 2003).

Can we distinguish between the alternative hypotheses of stellar versus miniquasar ionization sources? One distinguishing feature is the intrinsic source spectrum, which is thermal for stars but with

*E-mail: saleem@astro.rug.nl

a cut-off at a few times the Lyman limit frequency, but power-law for miniquasars with a spectrum that extends to high energies with nearly equal logarithmic increments in energy per decade of frequency. We show here that there is a dramatic difference between these two cases in the widths of the ionization fronts. Only the miniquasar model translates to scale-dependent 21-cm brightness temperature fluctuations that should be measurable by the Low-Frequency Array telescope (LOFAR).

2 WIDTH OF X-RAY IONIZATION FRONTS

Typically, the spectrum of the ultraviolet radiation of stellar sources is roughly flat with a cut-off at a few times the Lyman limit frequency. This results in a very sharp transition from ionized to neutral IGM. The thickness of such a region may be estimated from the mean free path of a photon with energy E within a neutral medium,

$$\langle l_E \rangle \approx \frac{1}{n_{\text{H}} \sigma_{\text{H}}(E)}, \quad (1)$$

where $n_{\text{H}} \approx 2.2 \times 10^{-7} \text{ cm}^{-3} (1+z)^3$ (Bennett et al. 2003) is the mean number density of hydrogen at a given redshift, and $\sigma_{\text{H}}(E) = \sigma_0 (E_0/E)^3$ is the bound-free absorption cross-section for hydrogen with $\sigma_0 = 6 \times 10^{-18} \text{ cm}^2$ and $E_0 = 13.6 \text{ eV}$. At $z = 10$, the mean free path for the most energetic photon from a stellar source is of the order of 0.1 comoving kpc.

In contrast, the power-law behaviour of the radiation specific intensity of miniquasars produces a much thicker ionization front. In the following calculation, we estimate this thickness assuming a uniform mass density distribution in which a miniquasar is embedded. This obviously does not take into account any mass or quasar clustering properties; however, for the purpose of exploring the thickness to within an order of magnitude and its qualitative evolution with redshift and dependence on the black hole mass, this assumption is acceptable. A more realistic numerical calculation will be carried out in the future.

We are also going to assume ionization–recombination equilibrium. This may be safely assumed for the photons in which we are interested as they have a mean free path of ≈ 1 –10 comoving Mpc at redshift ≈ 10 –5, which translates to a mean scattering time of about 0.5 – 5×10^6 yr, much less than a Hubble time at the relevant redshift range.

The miniquasar source spectrum is taken to be

$$I(E) = AgE^{-0.8} e^{-E/E_c} \text{ cm}^{-2} \text{ s}^{-1}, \quad (2)$$

where g is the Gaunt factor and A is normalized such that the luminosity of the miniquasar is $10^{43} \mu \text{ erg s}^{-1}$, for black holes of mass $10^5 \mu M_{\odot}$, with $1 \lesssim \mu \lesssim 10^3$, and the cut-off energy E_c is 200 keV (Sazonov, Ostriker & Sunyaev 2004). This translates to a number of ionizations at a distance r from the source,

$$\mathcal{N}(E; r) = e^{-\tau(E; r)} \frac{Ag}{(r^2/\text{Mpc}^2)} E^{-0.8} \left(\frac{E}{E_i} \right) e^{-E/E_c}, \quad (3)$$

with

$$\tau(E; r) = \int_0^r n_{\text{H}} x_{\text{H}} \sigma(E) dr. \quad (4)$$

Here x_{H} is the hydrogen neutral fraction.

The factor E/E_i in equation (3) is added to account for the mean number of ionizations per ionizing photon with $E_i \approx 36 \text{ eV}$. This last choice is a simplifying approximation to the number of ionizations per photon, which has a more complex dependence on energy and ionized fraction of hydrogen (Shull & van Steenberg 1985; Dijkstra

et al. 2004). The approximation that we adopt here is reasonable for photons within the energy range that gives rise to the thickness of the ionization front, i.e. photons with $E \approx 0.2$ –1 keV.

The cross-section quoted earlier does not take into account the presence of helium. In order to include the effect of helium, we follow Silk et al. (1972) who modified the cross-section to become

$$\sigma(E) = \sigma_{\text{H}}(E) + \frac{n_{\text{He}}}{n_{\text{H}}} \sigma_{\text{He}} = \sigma_1 \left(\frac{E_0}{E} \right)^3. \quad (5)$$

A proper treatment of the effect of helium is accounted for by defining σ_1 to be a step function at the two helium ionization energies corresponding to He I and He II. This, however, includes lengthy calculations and complicates the treatment, and we therefore choose σ_1 to be a smooth function of E , an approximation that will overestimate $\sigma(E)$ for low-energy photons. For photons with the relevant energy range, namely those responsible for creating the thick transition layer, this is a reasonable assumption.

The equation of ionization equilibrium which expresses the balance between the rate of ionization and recombination events is

$$\alpha_{\text{H}}^{(2)} n_{\text{H}}^2 (1 - x_{\text{H}})^2 = \Gamma(E; r) n_{\text{H}} x_{\text{H}} \left(1 + \frac{\sigma_{\text{He}} n_{\text{He}}}{\sigma_{\text{H}} n_{\text{H}}} \right). \quad (6)$$

Here $\Gamma(E; r)$ is the ionization rate per hydrogen atom for a given photon energy at distance r from the source. Since we are interested in the detailed structure of the ionization front, Γ is calculated separately for each r using the expression

$$\begin{aligned} \Gamma(E; r) &= \int_{E_0}^{\infty} \sigma(E) \mathcal{N}(E; r) \frac{dE}{E} \\ &= \frac{Ag \sigma_1}{3(r^2/\text{Mpc}^2)} \frac{E_0^{0.2}}{E_i} \\ &\quad \times \int_0^1 y^{1/15} \exp \left[-\tau_0(r) y - \frac{E_0}{E_c} y^{-1/3} \right] dy, \end{aligned} \quad (7)$$

where we have introduced the following simplifying notation: equation (4) is written as $\tau(E; r) \equiv \tau_0(r) (E_0/E)^3$ where $\tau_0(r)$ is the optical depth for photons with the Lyman limit frequency at a given r . We also changed the integration variable to $y \equiv (E_0/E)^3$. $\alpha_{\text{H}}^{(2)}$ is the recombination cross-section to the second excited atomic level and has the values of $2.6 \times 10^{-13} T_4^{-0.85} \text{ cm}^3 \text{ s}^{-1}$, with T_4 , the gas temperature in units of 10 000 K, assumed here to be unity.

Fig. 1 shows the solution of equation (6) for miniquasars with various luminosities and different redshifts. The transition from neutral to ionized IGM is extended and has two features. The first is a sudden steep increase in the neutral fraction with a typical width of 5–10 comoving megaparsecs (see left-hand panel). The second feature is a wing which represents a much slower transition from $x_{\text{H}} \approx 0.8$ to 1. In the next section, we will show that with LOFAR one should be able to resolve both features for the luminous miniquasars. For the less luminous quasars, one might have a chance of just detecting the wing feature with LOFAR. Only a radio telescope like the Square Kilometer Array (SKA) that has 10 times the total collecting area of LOFAR will be able to see the whole transition down to miniquasars with $10^{43} \text{ erg s}^{-1}$ luminosity.

3 LOFAR PREDICTIONS

In radio astronomy, where the Rayleigh–Jeans law is usually applicable, the radiation intensity $I(\nu)$ is expressed in terms of the

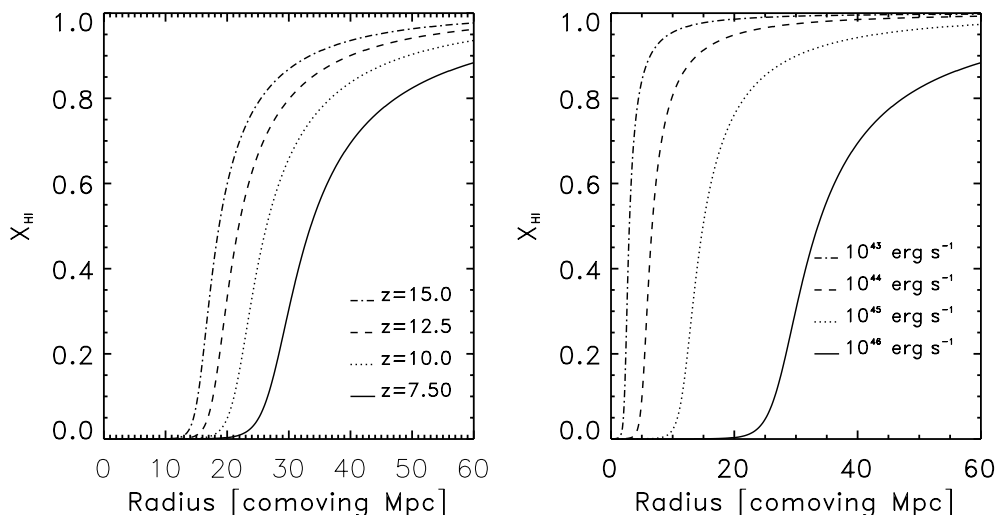


Figure 1. The left-hand panel shows the HI fraction as a function of comoving distance from the source for redshift values of $z = [7.5, 10, 12.5, 15]$ for a source with $\mu = 10^3$ in units of the Eddington luminosity for a $10^5 M_\odot$ black hole. The right-hand panel is similar to the left-hand one except that here the redshift is fixed to $z = 7.5$ and the various curves reflect values of $\mu = 1, 10, 100$ and 1000 .

brightness temperature, so that

$$I(\nu) = \frac{2\nu^2}{c^2} k T_b, \quad (8)$$

where ν is the radiation frequency, c is the speed of light and k is Boltzmann's constant (Rybicki & Lightman 1979). This in turn can only be detected differentially as a deviation from T_{CMB} , the cosmic microwave background temperature. The predicted differential brightness temperature deviation from the cosmic microwave background radiation is given by (Field 1958, 1959; Ciardi et al. 2003)

$$\delta T_b = 16 \text{ mK } x_{\text{HI}} \left(1 - \frac{T_{\text{CMB}}}{T_s} \right) \left(\frac{\Omega_b h^2}{0.02} \right) \left[\left(\frac{1+z}{10} \right) \left(\frac{0.3}{\Omega_m} \right) \right]^{1/2}. \quad (9)$$

Here T_s is the spin temperature and Ω_m and Ω_b are the mass and baryon density in units of critical density. In the following calculation, we take T_s to be significantly larger than T_{CMB} . The enhancement in T_s relative to T_{CMB} could be caused by the X-ray photons of the miniquasar itself or by an X-ray background produced collectively by miniquasars formed at higher redshifts (Tozzi et al. 2000; Ricotti & Ostriker 2004a; Nusser 2005). Furthermore, we are adopting a standard universe with a flat geometry, $\Omega_b h = 0.02$, $\Omega_m = 0.3$ and $\Omega_\Lambda = 0.7$.

Currently, there are a few experiments [e.g. LOFAR, the Primeval Structure Telescope (PAST) and the Mileura Widefield Array (MWA)] that are being designed to measure directly δT_b of the HI 21-cm hyperfine line and probe the physics of the reionization process by observing the neutral fraction of the IGM as a function of redshift. In this study we focus on predictions for LOFAR, but our conclusions could be easily applied to the other telescopes.

The LOFAR array consists geographically of a compact core area and 45 remote stations. Each remote station will be equipped with 100 High Band antennas and 100 Low Band antennas. In the core area, with 2-km diameter, there will probably be 32 substations. For the astronomy application, there will be a total of 3200 High Band and 3200 Low Band antennas in the core area. Currently, the planned maximum baseline between the remote stations is roughly 100 km. The Low Band antenna will be optimized for the 30–80 MHz

range while the High Band antenna will be optimized for the 120–240 MHz range.

The High Band antennas are sensitive enough to allow for the detection of the brightness temperature produced by the high-redshift 21-cm transitions. In this band, LOFAR will have the ability to measure brightness fluctuations as low as 5 mK with a spectral resolution of ≈ 1 MHz and a spatial resolution of about 3 arcmin. As currently configured, LOFAR will be sensitive to the 21-cm emission at redshift 6–11.5 over a field of 100 deg². First operation is foreseen towards the end of 2006.

The resolution of LOFAR depends on the telescope baseline and observed wavelength. As currently designed, the epoch of ionization signal will be sensitively measured mainly in the LOFAR core which has a FWHM resolution of ≈ 3 arcmin. For more information, see the LOFAR web site: <http://www.lofar.org>.

Here we have convolved the predicted brightness temperature fluctuations with the LOFAR beam, taking a Gaussian beam of FWHM 3 arcmin, and obtained the results shown in Fig. 2. This figure shows the expected LOFAR observed differential brightness temperature for various values of redshift with a fixed central black hole mass of $10^8 M_\odot$ (left-hand panel) and for different values of black hole mass with fixed redshift (right-hand panel). It is clear that the ionization front for the $\mu = 100$ – 1000 case is larger than the beam FWHM and could be easily observed with LOFAR. However, this is not the case for a miniquasar with central black hole mass $\lesssim 10^6 M_\odot$. The LOFAR baseline will allow higher resolution observations, but for those baselines the collecting area of the telescope with respect to the core increases very little, e.g. a baseline of 5 km has about 1.2 times the core collecting area, resulting in a sharp decrease in the telescope sensitivity at these resolutions. To resolve such ionization fronts fully, one would have to wait for e.g. the SKA which for the same baseline has an order of magnitude higher sensitivity than LOFAR. The extended wings of the ionized region shown in Figs 1 and 2 could also be observed with LOFAR, possibly even for the low-power miniquasars. These correspond to a small but not negligible ionized fraction ($x_{\text{HI}} \gtrsim 0.8$) with a δT_b of the order of a few. The extended region of these low-ionization wings compensates for their low signal and might possibly render them observable with LOFAR.

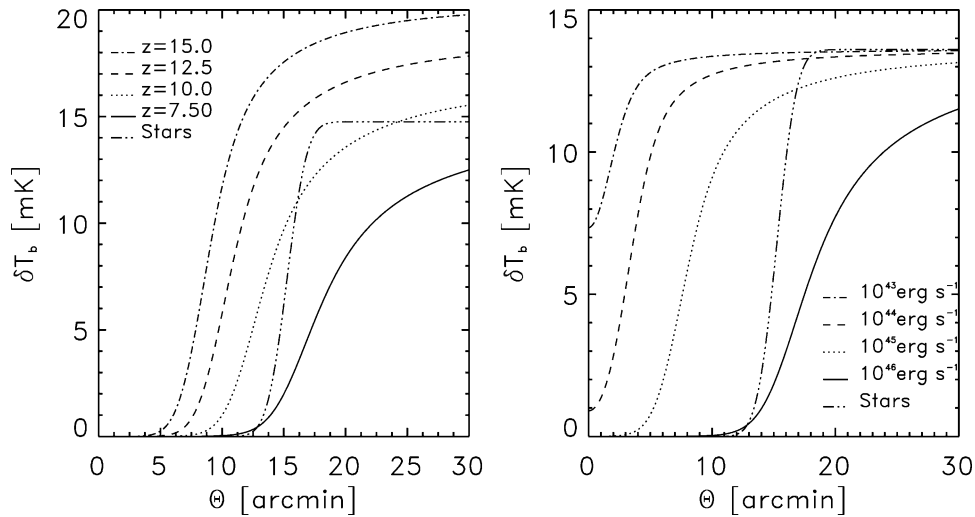


Figure 2. The left-hand panel shows δT_b convolved with the 3 arcmin FWHM LOFAR Gaussian beam as a function of angle from the source centre in arcmin for redshift values of $z = [7.5, 10, 12.5, 15]$ for a source with $\mu = 10^3$ corresponding to a central black hole mass of $10^8 M_\odot$. The right-hand panel is similar to the left-hand one except that here the redshift is fixed to $z = 7.5$ and the various curves reflect values of $\mu = 1, 10, 100$ and 1000 . The ionization front convolution corresponding to a Strömgren sphere, e.g. sharp ionization front appropriate for (stellar) thermal sources, at $z = 7.5$ is shown as well.

4 SUMMARY

In this paper we have shown that, for very simple assumptions, LOFAR could in principle indicate whether a certain ionization front is caused by miniquasars or stars by measuring its width. Our assumptions include a single spherical symmetric ionization source with no overlapping ionized spheres, a single ionizing population and a homogeneous background with no clustering. In the future, we will include the source clustering effects and the effects of the source luminosity function, and compute the LOFAR correlation function.

In reality, however, the reionization process might have been much more complex and have been induced by multiple types of ionization radiation sources that were dominant at various stages of the history of the Universe and present in an inhomogeneous medium. For example, massive Population III stars might die early on and create miniquasars that can maintain the IGM partially ionized through their hard photons (Ricotti & Ostriker 2004a,b; Madau et al. 2004), while the full ionization could be attributed to the soft miniquasar photons at later stages. Notwithstanding the complex ionization history of the IGM, the thickness of the ionization fronts expected to be observed via the 21-cm experiments [e.g. LOFAR and PAST (Peterson et al. 2004)] should still be a very strong discriminator between stellar and accreting black hole ionizing radiation sources.

ACKNOWLEDGMENTS

JS acknowledges the hospitality of the Kapteyn Astronomical Institute. The authors thank A. G. de Bruyn and P. Madau for discussions.

REFERENCES

Abel T., Bryan G. L., Norman M. L., 2000, *ApJ*, 540, 39
 Abel T., Bryan G. L., Norman M. L., 2002, *Sci*, 295, 93
 Avelino P. P., Liddle A. R., 2004, *MNRAS*, 348, 105
 Bennett C. L. et al., 2003, *ApJS*, 148, 1
 Bromm V., Kudritzki R. P., Loeb A., 2001, *ApJ*, 552, 464
 Bromm V., Coppi P. S., Larson R. B., 2002, *ApJ*, 564, 23
 Cen R., 2003, *ApJ*, 591, L5

Ciardi B., Ferrara A., White S. D. M., 2003, *MNRAS*, 344, L7
 Croft R. A. C., Weinberg D. H., Bolte M., Burles S., Hernquist L., Katz N., Kirkman D., Tytler D., 2002, *ApJ*, 581, 20
 Daigne F., Olive K. A., Vangioni-Flam E., Silk J., Audouze J., 2004, *ApJ*, 617, 693
 Dijkstra M., Haiman Z., Loeb A., 2004, *ApJ*, 613, 646
 Fan X., Narayanan V. K., Strauss M. A., White R. L., Becker R. H., Pentericci L., Rix H., 2002, *AJ*, 123, 1247
 Ferrarese L., 2002, *ApJ*, 578, 90
 Ferrarese L., Merritt D., 2000, *ApJ*, 539, L9
 Field G. B., 1958, *Proc. IRE*, 46, 240
 Field G. B., 1959, *ApJ*, 129, 551
 Gebhardt K. et al., 2000, *ApJ*, 543, L5
 Haiman Z., Holder G. P., 2003, *ApJ*, 595, 1
 Hui L., Haiman Z., 2003, *ApJ*, 596, 9
 Islam R. R., Taylor J. E., Silk J., 2003, *MNRAS*, 340, 647
 Kogut A. et al., 2003, *ApJS*, 148, 161
 Madau P., Rees M. J., 2001, *ApJ*, 551, L27
 Madau P., Rees M. J., Volonteri M., Haardt F., Oh S. P., 2004, *ApJ*, 604, 4
 Nusser A., 2005, *MNRAS*, 359, 183
 Oh S. P., 2000, PhD Thesis, Princeton University
 Oh S. P., 2001, *ApJ*, 553, 499
 Peterson J. B., Pen U.-L., Wu X.-P., 2004, *Mod. Phys. Lett. A*, 19, 1001
 Ricotti M., Ostriker J. P., 2004a, *MNRAS*, 350, 539
 Ricotti M., Ostriker J. P., 2004b, *MNRAS*, 352, 547
 Rybicki G. B., Lightman A. P., 1979, *Radiative Processes in Astrophysics*. John Wiley & Sons, Inc., New York
 Sazonov S. Y., Ostriker J. P., Sunyaev R. A., 2004, *MNRAS*, 347, 144
 Schaerer D., 2002, *A&A*, 24, 337
 Shull J. M., van Steenberg M. E., 1985, *ApJ*, 298, 268
 Silk J., Goldsmith D. W., Field G. B., Carrasco L., 1972, *A&A*, 20, 287
 Sokasian A., Abel T., Hernquist L., Springel V., 2003, *MNRAS*, 344, 607
 Somerville R., Livio M., 2003, *ApJ*, 593, 611
 Spergel D. N. et al., 2003, *ApJS*, 148, 175
 Sugiyama N., Zaroubi S., Silk J., 2004, *MNRAS*, 354, 543
 Theuns T., Schaye J., Zaroubi S., Kim T., Tzanavaris P., Carswell B., 2002, *ApJ*, 567, L103
 Tozzi P., Madau P., Meiksin A., Rees M. J., 2000, *ApJ*, 528, 597
 Walter F., Carilli C., Bertoldi F., Menten K., Cox P., Lo K. Y., Fan X., Strauss M. A., 2004, *ApJ*, 615, L17
 Wyithe J. S. B., Loeb A., 2004, *Nat*, 427, 815

This paper has been typeset from a $\text{\TeX}/\text{\LaTeX}$ file prepared by the author.